ILMU KELAUTAN: Indonesian Journal of Marine Sciences *September 2026 Vol 31(3):253-264* *e-ISSN 2406-7598*

Variability of Ocean Circulation and Water Mass Characteristics in Celebes Sea during ENSO Phase: A Numerical Modelling Approach

Rizqi Rizaldi Hidayat[1]*, Isnaini Prihatiningsih[1], Amir Yarkhasy Yuliardi[1], Sentana Wahyu Saputra[1], Muhammad Zainuddin Lubis[2], Ferdy Gustian Utama[3]

[1]Department of Marine Science, Faculty of Fisheries and Marine Sciences, Jenderal Soedirman University
Jl. Dr Soeparno, Karangwangkal Purwokerto Utara, Banyumas, Jawa Tengah 53122 Indonesia
[2]College of Oceanography and Ecological Science, Shanghai Ocean University
Shanghai 201306, China
[3]Low Latitude Climate Variability, MARUM, University of Bremen
Leobener Str.8, 28359 Bremen, Germany
Email: rizqi.rizaldi@unsoed.ac.id

Abstract

A three-dimensional regional ocean circulation simulation was conducted in the Celebes Sea using the Coastal and Regional Ocean Community Model (CROCO) with a spatial resolution of 1/16°. The simulation covered the period from 2015 to 2020, encompassing several contrasting El Niño–Southern Oscillation (ENSO) conditions. These included the strong El Niño event in 2015, the weak La Niña event in 2018, and the moderate La Niña event in 2020. Model performance was evaluated by comparing the simulation results with Argo observations and satellite altimetry data. The comparison showed a good agreement between the model and observations, with correlation coefficients ranging from 0.70 to 0.99. The results indicated that ENSO events substantially influenced ocean circulation and water mass characteristics in the Celebes Sea. During the 2015 El Niño event, seasonal current velocities generally weakened, while the surrounding waters became cooler and more saline. In contrast, during the 2018 and 2020 La Niña events, current velocities tended to increase, particularly within the thermocline layer. The La Niña conditions were also associated with relatively warmer and fresher waters. These changes were especially evident around the inflow and outflow regions of the Indonesian Throughflow, where variations in water properties and circulation were more pronounced. Overall, the simulation demonstrates that ENSO variability plays an important role in controlling the temporal changes in circulation and water mass properties within the Celebes Sea. The contrasting responses observed during El Niño and La Niña highlight the strong connection between large-scale climate variability and regional oceanographic processes in this important Indonesian marginal sea.

Keywords: *Celebes Sea, ITF, CROCO model, ENSO*

Introduction

The Sulawesi Sea (Celebes Sea) is a deep-water basin exceeding 5,000 meters and serves as the primary conduit for the Indonesian Throughflow (ITF). The ITF transports water masses from the Pacific Ocean to the Indian Ocean, driven by the sea surface height difference between the two oceans (Giu *et al*., 2020; Wahyuni *et al*., 2024; Li *et al*., 2025). According to Fine *et al*. (1994), the ITF originates from the Mindanao Current, a component of the North Equatorial Current (NEC). Gordon *et al.* (2012) further indicate that approximately 80% of the ITF water mass flows through the Celebes Sea toward the Makassar Strait. This dominant pathway plays a pivotal role in regional oceanographic dynamics, shaping circulation patterns, salinity and temperature distribution, and nutrient transport (Vinayachandran *et al*., 2021; Lubis *et al*., 2025; Putra *et al*., 2025). Although the Celebes Sea plays a strategic role in the ITF system, the understanding of its three-dimensional vertical circulation structure and water mass characteristics remains limited. This is particularly evident when compared with studies that have been conducted in neighboring regions, such as the Maluku Sea and Halmahera Sea. (Suryadarma *et al*., 2025; Lubis *et al*., 2026).

The transport of water masses by the ITF is influenced by global and regional climate variability. On a seasonal scale, monsoon winds affect the strength of the ITF, intensifying it during the east monsoon and weakening it during the west monsoon (Peña-Molino *et al*., 2022; Zhu and Wang, 2024). On an interannual scale, phenomena such as El Niño, La Niña, and the Indian Ocean Dipole (IOD) impact the volume of ITF transport. The El Niño phase weakens the current, whereas La Niña strengthens it (Giu *et al*., 2020; Zhang *et al*., 2023). This variability also affects the characteristics of water masses along the ITF pathway, which in turn influences ecosystems, biodiversity, and human activities such as fisheries

*) Corresponding author

https://ejournal.undip.ac.id/index.php/ijms
DOI: 10.14710/ik.ijms.31.3.253-264
Received : 25-04-2026
Accepted : 26-06-2026

and shipping. Interannual modulation of the ITF by ENSO alters not only transport magnitude but also vertical structure and thermohaline properties, particularly within the thermocline layer that dominates the ITF core flow (Wei *et al*., 2025).

During the period 2015-2020, various global climate phenomena influenced the dynamics of the Celebes Sea. The strong El Niño event of 2015-2016 increased sea surface temperatures in the central Pacific Ocean and altered trade wind patterns (Santoso *et al*., 2017; Yang *et al*., 2022). Subsequently, the weak La Niña Modoki in 2016-2017 raised Indonesian sea surface temperatures, while the moderate La Niña in 2020-2021 strengthened northeast trade winds and increased rainfall across much of Indonesia (Lestari *et al*., 2019; Alfiqri *et al*., 2024). The fluctuating climatological conditions throughout this 2015-2020 period have the potential to affect circulation variability and water mass characteristics in the Celebes Sea. This period therefore provides a natural laboratory to examine the oceanic response to contrasting ENSO phases within a relatively short but dynamically diverse timeframe.

Despite the recognized role of ENSO in modulating the ITF, the three-dimensional variability of circulation and water mass characteristics in the Celebes Sea remains poorly understood, particularly during contrasting ENSO phases. High-resolution modeling studies focusing on this region are still scarce. To address this gap, this study employs a high-resolution three-dimensional ocean model to examine the influence of ENSO on the circulation patterns and water mass variability of the Celebes Sea during 2015–2020. By resolving both horizontal and vertical ocean dynamics, the study provides new insights into the physical mechanisms underlying oceanographic variability and their broader implications for the regional marine system.

Materials and Methods

The study area encompasses the Celebes Sea basin and its surrounding interconnected regions. To the north, the model domain is bounded by the Sulu Sea, while the southern boundary includes the entrances to the Makassar Strait and the Maluku Sea. The eastern boundary covers the region connecting the Celebes Sea to the western Pacific Ocean. This domain configuration is designed to capture the major pathways of water mass exchange that influence circulation dynamics within the Sulawesi Sea. Numerical simulations were conducted over a six year period, from January 1, 2015, to December 31, 2020, thereby encompassing both El Niño and La Niña phases. In this study, observation points were established at three locations representing the primary pathways of water mass exchange. These points correspond to the Sulu Sea inflow, the Pacific inflow to the ITF, and the Makassar Strait outflow, enabling a focused analysis of circulation and water mass transformation along the ITF pathway (Figure 1).

Data sources and model inputs

Several observational and reanalysis datasets were used to construct, force, and evaluate the CROCO model simulations. Bathymetric information was obtained from the General Bathymetric Chart of the Oceans (GEBCO), which provides global topographic data at a spatial resolution of 15 arc-seconds based on the SRTM15+ dataset (Thuillier *et al*., 2024).

Atmospheric forcing fields were derived from the ERA5 reanalysis product, including both single-level and pressure-level variables with an hourly temporal resolution and a horizontal resolution of 0.25° × 0.25°. Initial and lateral boundary conditions were obtained from the GLORYS12V1 global ocean reanalysis dataset, which provides three-dimensional oceanographic fields at a spatial resolution of 0.0833° and daily temporal outputs. Tidal forcing was generated from the TPXO7 global tidal model, consisting of 11 major tidal constituents (M2, S2, N2, K2, K1, O1, P1, Q1, MM, MF, and M4) with a spatial resolution of 0.25° × 0.25° (Tian *et al*., 2024).

To evaluate model performance, simulated oceanographic variables were compared with independent observations from Argo profiling floats and satellite altimetry products. These datasets were used to assess the model's ability to reproduce the observed hydrographic structure and sea surface variability in the Celebes Sea.

Model configuration

The Coastal and Regional Ocean Community Model (CROCO) version 1.3 was employed to investigate the variability of ocean circulation and water mass characteristics in the Celebes Sea during 2015-2020. The model domain covers the Celebes Sea and adjacent waters, extending from 117.06°E to 126.12°E and from 0.31°S to 7.98°N. The model was configured with a horizontal resolution of 1/16° (~6.2 km) and 40 vertical sigma-coordinate layers.

Bathymetry was derived from the GEBCO dataset and smoothed using an r-factor of 0.15 to reduce pressure-gradient errors and improve numerical stability. The vertical coordinate system was defined using stretching parameters of $\theta s = 7$, $\theta b = 2$, and $hc = 200$ m, providing enhanced vertical resolution in the upper ocean where strong gradients of temperature and salinity occur.

Model simulations were conducted from 1 January 2015 to 31 December 2020. The first year (2015) was treated as a spin-up period to allow the model to reach a dynamically balanced state before analysis. Model integration was performed using a hot-start approach, in which the model state at the end of the spin-up period (2015) was used as the initial condition for the main simulation (2016-2020). Additional details of the numerical configuration, including grid dimensions, vertical discretization, and time-stepping parameters, are summarized in Table 1. The model generated daily average fields of sea surface height, current velocity, temperature, and salinity. These outputs were subsequently analyzed to investigate seasonal and interannual variability associated with different ENSO phases in the Celebes Sea.

Data analysis

The mean and variance were calculated and visualized from January 2015 to December 2020 to highlight the largest fluctuations in the model outputs across the Celebes Sea region. To ensure the accuracy and reliability of the model, simulated temperature and salinity values were validated against Argo float measurements, while sea level anomalies were validated using satellite altimetry observations.

Water mass circulation in the Celebes Sea was analyzed using modeled current results across three distinct water mass layers. The depths of these layers were determined based on water mass stratification thresholds. The mixed layer was defined by criteria of $\Delta T < 0.1°C$ and $\Delta\sigma\theta < 0.02$ kg/m³, whereas the thermocline layer met $\Delta T \geq 0.1°C$ and $\Delta\sigma\theta \geq 0.02$ kg/m³ (Prihatiningsih *et al*., 2021). After identifying the vertical extent of each layer across all seasons and locations, representative depth levels were selected to represent the mixed layer, thermocline, and deep layer, respectively, thereby facilitating a comparison of circulation patterns across ENSO phases.

Observations were conducted during the western and eastern monsoon seasons across years representing different ENSO (El Niño–Southern Oscillation) conditions. The selected years were determined based on the Oceanic Niño Index (ONI), with 2015 representing a strong El Niño event Santoso *et al*. (2017), while 2018 and 2020 representing weak and moderate La Niña conditions, respectively (Alfiqri *et al*., 2024). The western monsoon season was represented by December, January, and February (DJF), whereas the eastern monsoon season was represented by June, July, and August (JJA). Vertical and temporal variations in temperature and salinity at the observation stations were analyzed and visualized using Hovmöller diagrams.

Pearson correlation analysis was used to quantify the relationship between ENSO variability and current velocity in the Celebes Sea. The analysis was performed using monthly ENSO index values and current velocity at representative depths of 5 m, 93 m, and 250 m, corresponding to the mixed layer, thermocline layer, and deep layer, respectively. To investigate the seasonal dependence of ENSO forcing, the correlation analysis was conducted separately for the northwest monsoon (DJF), first transition season (MAM), southeast monsoon (JJA), and second transition season (SON). Correlation coefficients (r) and associated p-values were calculated to evaluate the strength and statistical significance of the relationships.

Model validation

The outputs of the CROCO model were validated against satellite observation data. Validation data were extracted from Sea Level Anomaly (SLA) points for the period 2015-2020 (Figure 1). The root mean square error (RMSE) and correlation coefficient (r) were computed between the model results and observational data. A correlation between coefficient value approaching one indicates strong agreement between the model outputs and observations.

Table 1. Main parameters used in the CROCO model configuration

Parameter	Value	Units	Description
LLm0	144	grid points	Number of horizontal grid points in the XI-direction
MMm0	132	grid points	Number of horizontal grid points in the ETA-direction
N	40	levels	Number of vertical sigma levels
dt	120	s	Baroclinic model time step
NFAST	80	dimensionless	Number of barotropic time steps per baroclinic time step
hc	200	m	Critical depth parameter of the vertical S-coordinate system
θs	7	dimensionless	Surface stretching parameter of the vertical S-coordinate system
θb	2	dimensionless	Bottom stretching parameter of the vertical S-coordinate system

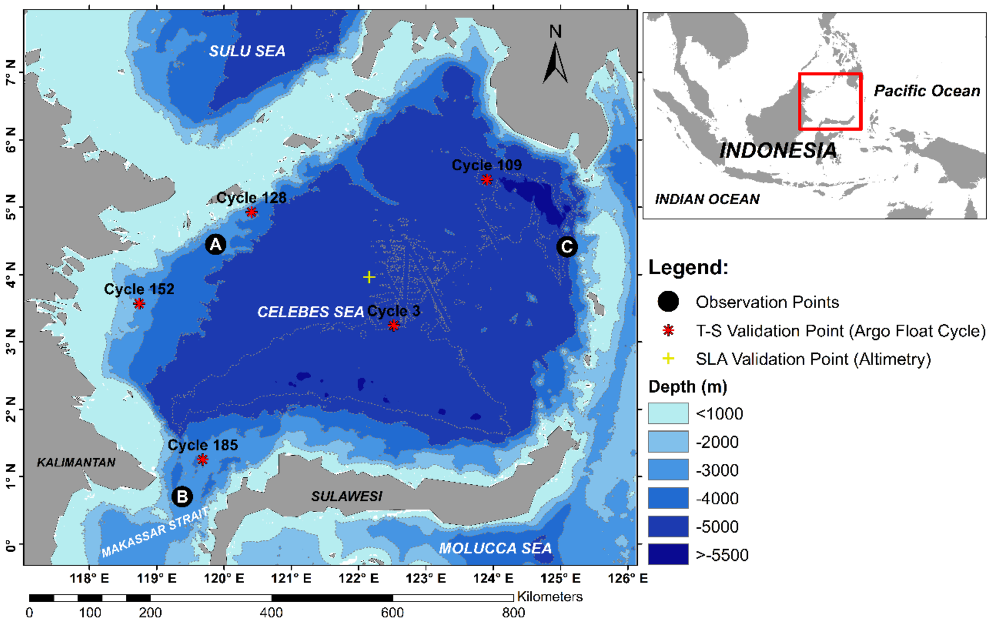

Figure 1. Study Area in Celebes Sea. Red stars and yellow plus signs indicate validation points, divided into temperature–salinity and SLA datasets. Observational data are shown as black dots. Point A represents the northern connection to the Sulu Sea, Point B the southern pathway to the Makassar Strait, and Point C the eastern opening toward the North Pacific.

The annual and seasonal SLA fluctuation patterns from the CROCO model closely follow those observed in the DUACS dataset, with some differences in amplitude during specific periods. For instance, during 2015-2016, both the CROCO model and DUACS data exhibit a sharp decline in SLA. From mid-2017 to early 2018, a significant increase in SLA is evident in both datasets. In contrast, late 2018 and late 2019 show a renewed decrease, though less pronounced than the 2015-2016 period. These rising and falling SLA patterns in both datasets are attributed to climatological fluctuations, particularly ENSO events that occurred throughout 2015-2020.

Figure 3 illustrates the comparison between model results and observational data for the three primary variables: SLA, temperature, and salinity. The correlation coefficients for all variables demonstrate a strong relationship, ranging from 0.7 to 0.99. This confirms that the CROCO model effectively reproduces fluctuations in sea level, temperature, and salinity driven by climatological changes, with commendable performance. Supporting this, the root mean square differences (RMSD) remain relatively low: less than 0.04 m for SLA, 2°C for temperature, and 0.38 PSU for salinity

Result and Discussion

The comparison between CROCO model simulation data and observational data (Argo floats) is presented in Figure 4. Model data were extracted from the grid point closest to the Argo float locations and adjusted to match the temporal and depth resolutions of the observations, ensuring comparability between the two datasets. Vertical profiles of temperature and salinity reveal a strong agreement in patterns between the CROCO model outputs and Argo float data, despite some deviations at certain depth ranges.

Across the entire cycle, the CROCO model's vertical temperature profiles exhibit consistent patterns with those from Argo floats, indicating the model's accuracy in replicating vertical temperature variability. In contrast, salinity profiles show discrepancies in specific cycles, such as cycles 3 and 152. These differences primarily occur in the surface layer, which is highly influenced by external factors including river runoff, precipitation, evaporation, and others. The overall consistency in vertical structures of temperature and salinity between model results and observations underscores the CROCO model's reliability in representing the water column conditions. Achieving high accuracy for these variables is crucial, as they are key to identifying circulation patterns and water mass characteristics in the study region.

Mean and variance of the oceanographic parameters

Observations of water mass circulation variability in the Sulawesi Sea were conducted using

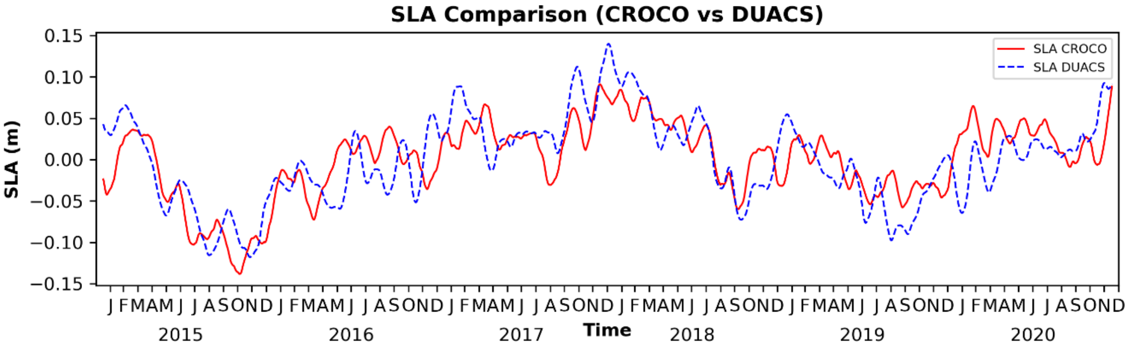

Figure 1. Comparison between SLA data from the CROCO model (red solid line) and observed SLA from DUACS (blue dashed line).

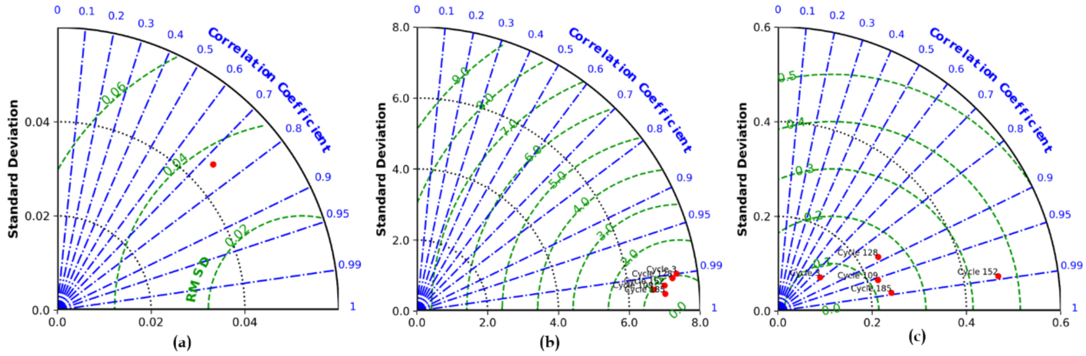

Figure 2. Taylor diagram parameters for (a) SLA, (b) temperature, and (c) salinity comparing model results with observational data.

modeled current results across three distinct water mass layers: the mixed layer (depth -5 m), the thermocline layer (-93 m), and the deep layer (-150 m) (Figure 4). The selection of these depths was based on water mass stratification using standard temperature and salinity thresholds (density difference >0.1 kg/m^3). The analysis focused on the west and east monsoon seasons during ENSO (El Niño-Southern Oscillation) years, namely 2015 (strong El Niño), 2018 (weak La Niña), and 2020 (moderate La Niña). The ENSO phenomenon plays a crucial role in modulating wind patterns and water mass circulation in the region.

In general, current patterns in the Celebes Sea exhibit clear seasonal differences. During the western monsoon, surface currents predominantly originate from the Sulu Sea, entering the area through the narrow Sulu Archipelago channels at high speeds of up to ~1 m.s^{-1}, and remain consistent throughout the season across all years. In contrast to the surface layer, thermocline currents from the Sulu Sea and Pacific Ocean exhibit similar speeds, except during the western monsoon of 2015 when Pacific currents were very weak (0-0.15 m.s^{-1}). This is associated with the strong El Niño event that year, which weakened the ITF transport along its pathway (Mahie, 2005). Conversely, during the western monsoon of 2018 (weak La Niña), thermocline currents from the Pacific reached the highest speeds compared to 2015 and 2020, driven by the enhancement of the warm pool in eastern Indonesia (Safitri *et al.*, 2012). Trisnakusumawati *et al.* (2022) further note that La Niña strengthens pressure gradients, leading to stronger trade winds and intensified currents relative to normal conditions.

During the eastern monsoon, inflows from the Pacific Ocean to the Sulawesi Sea tend to increase in speed, consistent with findings by Atmadipoera *et al.* (2016) that ITF transport through the Makassar Strait is stronger in this season compared to the western monsoon. In contrast, inflows from the Sulu Sea decrease, influenced by dominant tropical monsoon winds that govern its circulation (Hapsari *et al.*, 2021). Variations in current direction and speed in the Sulawesi Sea are also affected by the Sulu Sea circulation patterns, which depend on seasonal wind changes.

The influence of ENSO on Pacific inflows to the Sulawesi Sea is particularly evident during the 2015-2020 period. During the strong El Niño of 2015, current speeds across all three layers reached their

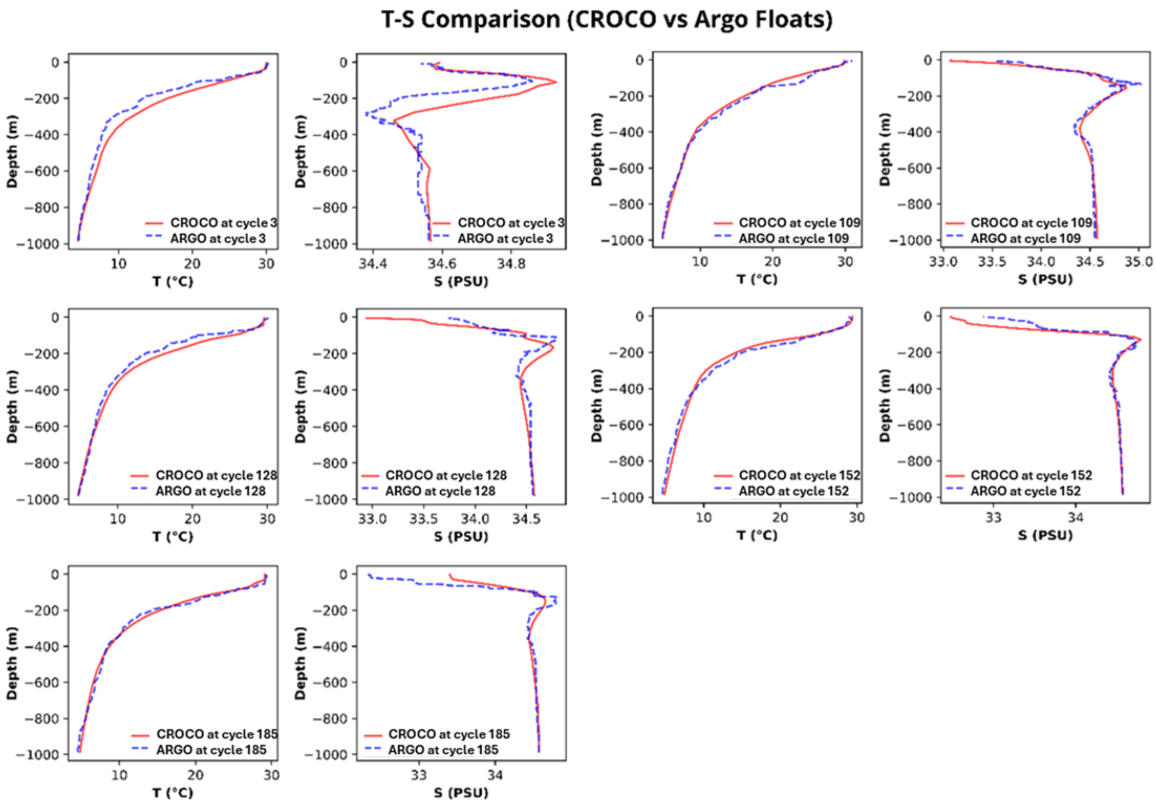

Figure 3. Comparison between the Croco model (red solid line) and Argo Floats (blue dashed line) including Cycle 3, Cycle 109, Cycle 128, Cycle 152, and Cycle 185

lowest values, while the moderate La Niña of 2020 resulted in stronger current speeds. Ratnasari *et al.* (2017) affirm that ENSO modulates current volume transport in Indonesian waters: weakening during El Niño and strengthening during La Niña. Analysis of means and variances indicates that the highest current speed variability occurred in the thermocline layer during ENSO transitions (standard deviation ~0.2-0.5 m.s^{-1}), reflecting the region's sensitivity to global climate variability.

Vertical and temporal variations of temperature and salinity

Figure 5 and Figure 6 illustrate the vertical and temporal distributions of modeled temperature and salinity at three key observation points: Point A (Sulu Sea - Sulawesi Sea connection), Point B (ITF outflow pathway), and Point C (ITF inflow pathway). Temperature (Figure 5) in the surface layer shows high values with significant fluctuations, whereas deeper layers tend to be lower and more stable. The fluctuations in surface temperature reflect direct influences from atmospheric variability, such as seasonal winds and solar radiation (Martin *et al*., 2021). According to (Suhana, 2018), surface seawater temperature is directly affected by several meteorological conditions, including wind speed, solar radiation intensity, humidity, evaporation, and rainfall. The stability and constancy of temperature in deeper layers result from minimal influence of currents operating at those depths (Sidabutar *et al*., 2014; Song *et al*., 2024).

At Point A, surface layer temperatures are generally higher compared to the other two points. Throughout 2015-2020, temperatures at Point A consistently ranged from 30-31°C, despite influences from climatological changes. This is attributed to the inflow of water masses with high-temperature characteristics from the Sulu Sea, which is directly connected to the South China Sea (Triyulianti *et al*., 2018). In contrast, at Point C, surface temperatures are more strongly influenced by climatological variability and the movement of water masses from the Pacific Ocean. During El Niño events, surface temperatures at Point C decrease, while they increase during La Niña events. Alfiqri *et al.* (2024) note that the Sulawesi Sea serves as an entry point for water masses from the Pacific Ocean, making its water mass characteristics highly susceptible to phenomena occurring in the Pacific, including ENSO. Meanwhile, temperatures at Point B fall between those at Points A and C. Over the 2015-

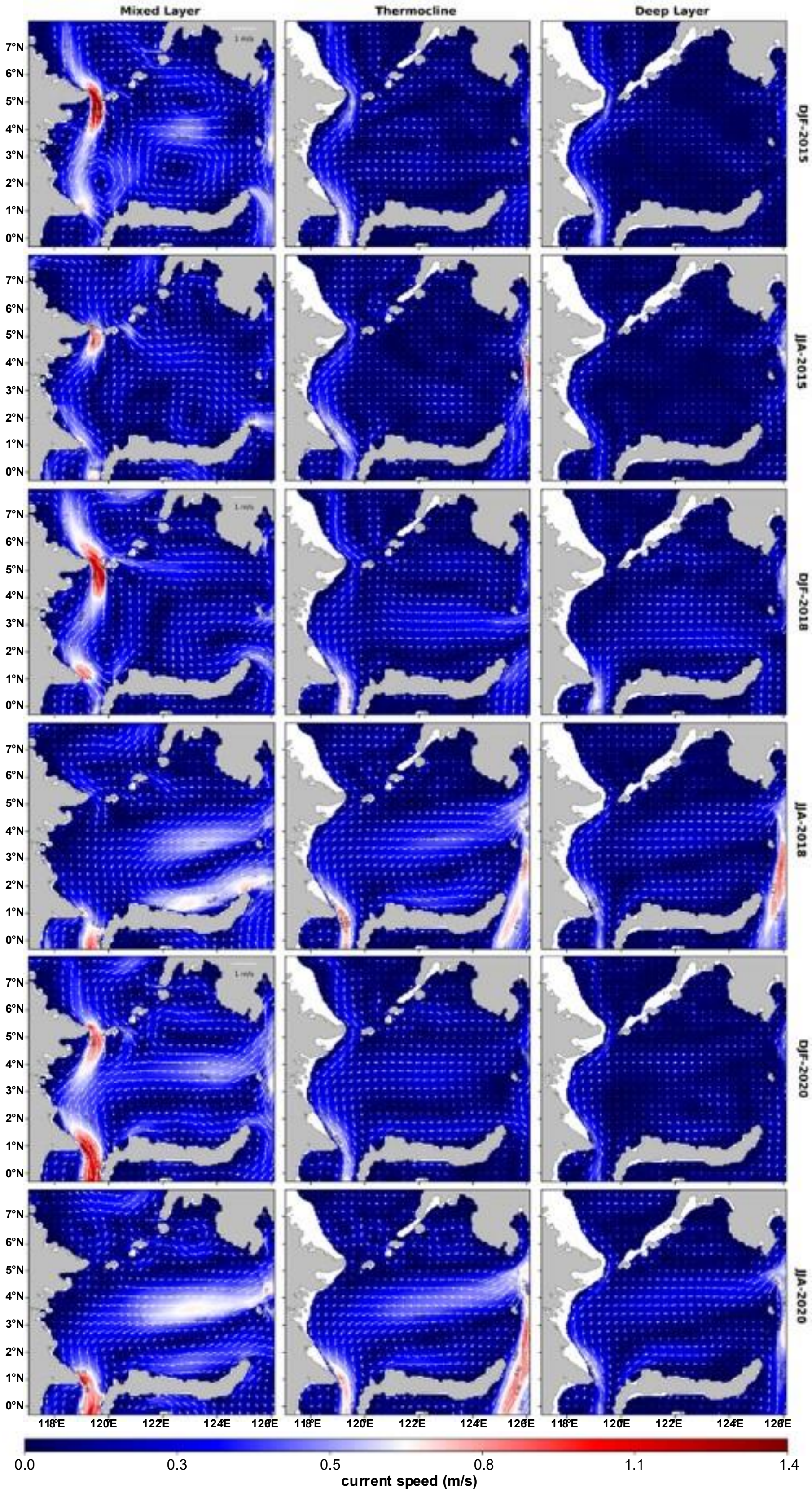

Figure 4. Seasonal mean spatial distribution (DJF representing the northwest monsoon and JJA representing the southeast monsoon) of currents in the Celebes Sea during ENSO years at the surface layer, thermocline layer, and deep layer, including: 2015 (El Niño phase), 2018 (La Niña phase), and 2020 (Netral phase).

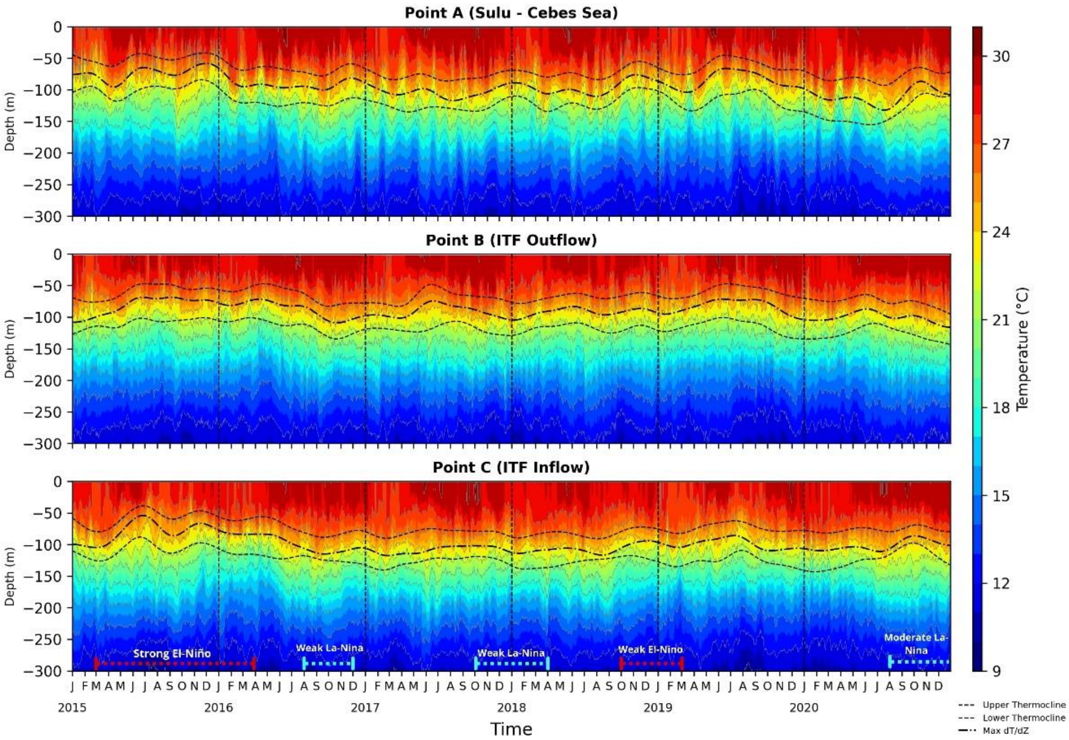

Figure 5. Hovmoller Diagram of vertical temperature with thermocline layer indicator line.

2020 period, surface temperatures at Point B showed moderate fluctuations, influenced by climatological changes but to a lesser extent than at Point C.

Temporally, temperatures at all depths fluctuate in response to climatological phenomena. During the strong El Niño of 2015-2016, warm water masses at all three points experienced shoaling, marked by an upward shift in the thermocline layer. As it transitioned to a weak La Niña phase in late 2016 and early 2018, warm water masses deepened compared to neutral conditions observed at the end of 2019. This deepening of warm water masses also occurred during the moderate La Niña phase at the end of 2020, with the thermocline layer positioned deeper than under neutral conditions. These vertical temperature distribution changes demonstrate that global climate variability, such as El Niño and La Niña, directly impacts water mass structure and temperature distribution in the Sulawesi Sea (Hadi *et al*., 2012; Hutabarat *et al*., 2018).

Regarding salinity, values at Point A (the region connecting the Sulawesi Sea to the Sulu Sea) are lower than at Point C (the ITF inflow region), particularly from 0 to 200 m depth. At the surface of Point A, salinity values ranging from 32.5-34.5 PSU are consistently distributed over time. The low salinity at Point A is due to the inflow of low-salinity water masses from the Sulu Sea into the Sulawesi Sea (Li and Zhang, 2023). Higher salinity episodes occur during short periods, such as the strong El Niño at the end of 2015, the transition phase following the strong El Niño in 2016, and the onset of a weak El Niño at the end of 2018.

At the surface layer of Point C, salinity values tend to fluctuate in response to climatological conditions. During the strong El Niño in 2015, surface salinity at Point C ranged from 33 to 34.8 PSU, whereas during the moderate La Niña at the end of 2020, it decreased to 33-33.9 PSU. High salinity values at Point C, ranging from 34.8 to 35 PSU, are widely distributed and consistently follow climatological changes. The tendency for higher and more fluctuating salinity at Point C is influenced by the inflow of water masses from the Pacific Ocean (Triyulianti *et al*., 2018; Toding *et al*., 2022).

At Point B (the ITF outflow gateway), salinity exhibits a unique pattern compared to Points A and C. In the surface layer (0 to -50 m), salinity values at Point B generally range between those at Points A and C, namely 33 to 34.5 PSU. This pattern remains relatively stable over time, with only minor fluctuations linked to global climatological changes such as El Niño and La Niña. Variations in Sulawesi Sea salinity at Point B may be caused by mixing processes of water masses (Yuliardi *et al*., 2022).

Table 2. Seasonal Pearson correlation coefficients (r) and significance levels (*P*) between the ENSO index and current velocity at different depth layers

Musim	5 m (r,*P*)	93 m (r,*P*)	250 m (r,*P*)
DJF	0.541 ; 0.020	0.094 ; 0.710	-0.631 ; 0.005
MAM	-0.343 ; 0.163	-0.475 ; 0.046	-0.449 ; 0.062
JJA	-0.330 ; 0.181	-0.629 ; 0.005	-0.698 ; 0.001
SON	-0.290 ; 0.242	-0.088 ; 0.728	-0.287 ; 0.248

** Values in bold represent significant correlations (*P *< 0.05).*

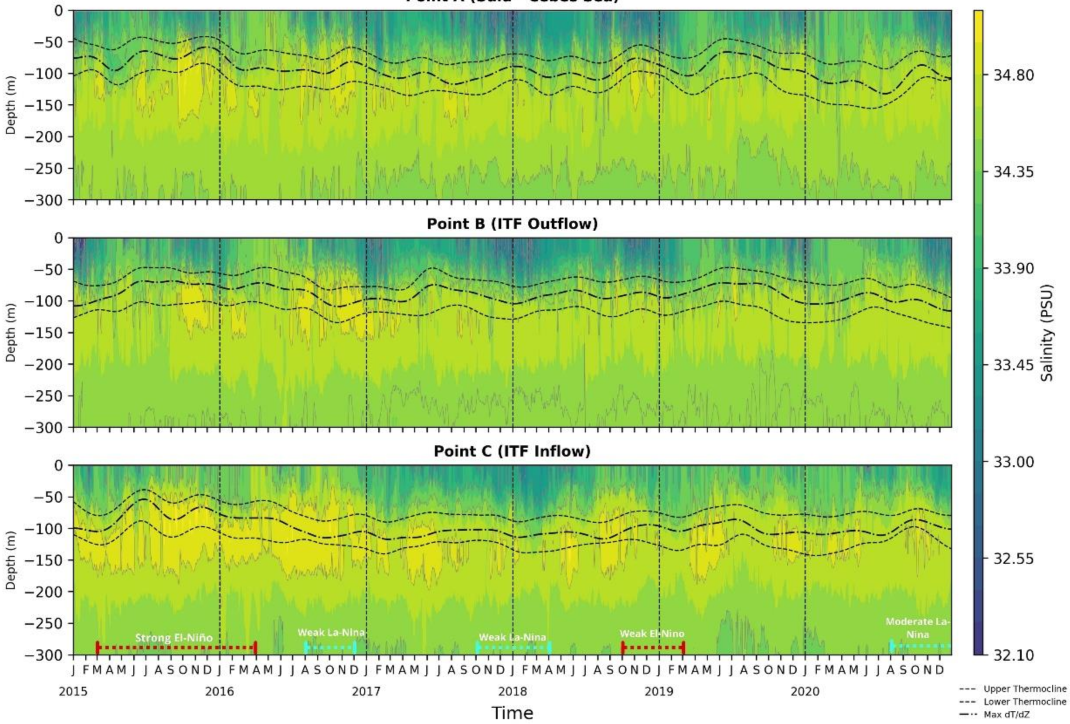

Figure 6. Hovmoller Diagram of vertical salinity with thermocline layer indicator line

Seasonal influence of ENSO on current velocity across different depth layers

The correlation analysis indicates that the influence of ENSO on current velocity in the Celebes Sea varies seasonally and becomes stronger with increasing depth. Significant correlations were mainly observed in the thermocline (93 m) and deep layer (250 m), whereas the surface layer (5 m) generally). These results indicate that El Niño conditions tend to weaken subsurface currents, while La Niña conditions strengthen them. Such behavior is consistent with the modulation of the ITF, which weakens during El Niño due to a reduced Pacific–Indian Ocean pressure gradient and intensifies during La Niña when the pressure gradient increases (Mao *et al*., 2025).

In contrast, the surface layer showed a significant positive correlation only during DJF (r = exhibited weaker relationships with ENSO variability. This pattern suggests that subsurface circulation is more responsive to large-scale climate forcing than surface circulation (Hariyadi *et al*., 2021).

The strongest ENSO signal occurred during the southeast monsoon (JJA), when significant negative correlations were found at 93 m (r = -0.629, *P* < 0.01) and 250 m (r = -0.698, *P* < 0.01) (0.541, *P* < 0.05), suggesting a stronger influence of seasonal monsoon forcing on near-surface circulation. The stronger correlations observed at 93 m and 250 m imply that ENSO variability is primarily transmitted through the thermocline and deeper layers, which represent the main pathway of ITF transport (Sprintall and Révelard, 2014). Overall, these findings show that the Celebes Sea circulation response to ENSO has a clear vertical structure, with the strongest influence in the subsurface layers during the southeast monsoon.

Conclusion

The CROCO 1/16° simulation results were successfully validated against satellite observations and Argo float data, demonstrating strong agreement in sea level, temperature, and salinity and confirming the robustness of the numerical framework. During 2015–2020, ENSO variability strongly influenced circulation and water-mass characteristics in the Celebes Sea. The strong El Niño in 2015 weakened current velocities, particularly within the thermocline layer, due to reduced ITF transport, whereas the moderate La Niña in 2020 enhanced current speeds through strengthened trade winds and warm pool development in eastern Indonesian waters. El Niño conditions were associated with lower temperatures and higher salinity, while La Niña phases exhibited higher temperatures and reduced salinity across all observation points. These coherent thermohaline responses highlight the close coupling between large-scale climate variability and local ocean dynamics. Overall, this study provides additional insights into the three-dimensional circulation and water mass variability of the Celebes Sea under contrasting ENSO conditions, emphasizing the value of high-resolution regional modeling for understanding upstream controls of the ITF and their implications for regional marine systems.

Acknowledgement

The authors would like to thank the Institute for Research and Community Service, Jenderal Soedirman University for the research grant from the Unsoed Basic Research Scheme (No. 14.368/UN23.34/ PT.01/V/2025).

References

Alfiqri, M.Z., Handoyo, G. & Widiaratih, R. 2024. Pengaruh El Niño 2015-2016 dan La Niña 2020-2021 terhadap SPL, klorofil-a, dan intensitas curah hujan di Laut Sulawesi. *Indon. J. Oceanog.*, 6(3): 239-248. https://doi.org/10.14710/ijoce.v6i3.20009

Atmadipoera, A., Horhoruw, S., Purba, M. & Nugroho, D. 2016. Variasi spasial dan temporal Arlindo di Selat Makassar. *J. Ilmu Teknol. Kelautan Tropis*, 8(1): 299-320. https://doi.org/10.29244/jitkt.v8i1.13221

Fine, R.A., Lukas, R., Bingham, F.M., Warner, M.J. & Gammon, R.H. 1994. The western equatorial Pacific: a water mass crossroads. *J. Geophys. Res.*, 99(C12): 25063-25080. https://doi.org/10.1029/94JC02277

Giu, L.O.M.G., Atmadipoera, A.S., Naulita, Y. & Nugroho, D. 2020. Struktur vertikal dan variabilitas Arlindo yang masuk ke tepi barat Laut Banda. *J. Ilmu Teknol. Kelautan Tropis*, 12(2): 457-472. https://doi.org/10.29244/jitkt.v12i2.29142

Hapsari, S.N., Syamsuddin, M.L., Riyantini, I. & Sunarto. 2021. Seasonal variations of sea surface temperature and sea current in the Celebes Sea. *World News of Natural Sci.*, 35: 135-143.

Hariyadi, H., Hutabarat, J., Sugianto, D.N., Noercholis, M.F.M., Prasetyarini, N.D., Pranowo, W.S., Kunarso, K., Wetchayount, P. & Wirasatriya, A. 2021. Natuna off-shelf current (NOC) vertical variability and its relation to ENSO in the North Natuna Sea. *Ilmu Kelautan: Indon, J. Mar. Sci.*, 26(2): 63-70. https://doi.org/10.14710/ik.ijms. 26.2.63-70

Hutabarat, M.F., Purba, N.P., Astuty, S., Syamsuddin, M.L. & Kuswardani, A.R.T.D. 2018. Variabilitas lapisan termoklin di Selat Makassar. *J. Perikanan dan Kelautan*, 9(1): 9-21.

Kunarso, Hadi, S., Ningsih, N.S. & Baskoro, M.S. 2012. Perubahan kedalaman dan ketebalan termoklin pada variasi kejadian ENSO, IOD dan Monsun di Perairan Selatan Jawa hingga Pulau Timor. *Ilmu Kelautan: Indon, J. Mar. Sci.*, 17(2): 87-98. https://doi.org/10.14710/ik.ijms.17.2.87-98

Lestari, D.O., Sutriyono, E., Kadir, S. & Iskandar, I. 2019. Impact of 2016 weak La Niña Modoki event over the Indonesian region. *Int. J. GEOMATE*, 17(61): 156-162. https://doi.org/10.21660/2019.61.8256

Li, A. & Zhang, Y. 2023. Long-term thermohaline trends in the Sulawesi Sea based on a high-resolution reanalysis data. *J. Phys. Conf. Ser.*, 2486(1). https://doi.org/10.1088/1742-6596/2486/1/012047

Li, A., Zhang, Y., Xu, T., Hong, M., Wang, Y. & Wu, J. 2025. The dominant role of the Indian Ocean Dipole in shaping the barotropic structure of Indonesian Throughflow outflow interannual variability: insights from the 2006-2007 positive Indian Ocean Dipole events. *Atmospheric and Oceanic Sci. Let.*, 100760. https://doi.org/10.1016/j.aosl.2025.100760

Lubis, M.Z., Hidayat, S. & Hu, S. 2025. Indonesian Throughflow in the Halmahera Sea: a review. *J. Mar. Sci. Eng.*, 13(10): 1974. https://doi.org/10.3390/jmse13101974

Lubis, M.Z., Hu, S., Simanjuntak, A.V.H., Dwinovantyo, A., Arnold, E.E.B., Kausarian, H., Jamjareegulgarn, P. & Suryadarma, M.W. 2026. How the interannual and seasonal variability in connectivity to ITF and its relation to ENSO events in the Halmahera Sea: a modeling approach and observation. *Reg. Stud. Mar. Sci.*, 94: 104792. https://doi.org/10.1016/j.rsma.2026.104792

Mahie, A.G. 2005. Model variasi transpor volume (Arlindo) hubungannya dengan ENSO (El Niño Southern Oscillation) di Selat Makassar. *J. Matematika, Statis. Komputasi*, 2(1): 8-16.

Mao, X., Zheng, S., Feng, M., Liang, P., Xie, L., Yang, L. & Yan, L. 2025. Interannual variability of the South Equatorial Current in the Southeast Indian Ocean associated with El Niño-Southern Oscillation. *J. Clim.*, 38(2): 545-562. https://doi.org/10.1175/JCLI-D-23-0725.1

Martin, P.E., Arbic, B.K. & Hogg, A.M. 2021. Drivers of atmospheric and oceanic surface temperature variance: a frequency domain approach. *J. Clim.*, 34(10): 3975-3990. https://doi.org/10.1175/JCLI-D-20-0557.1

Peña-Molino, B., Sloyan, B.M., Nikurashin, M., Richet, O. & Wijffels, S.E. 2022. Revisiting the seasonal cycle of the Timor Throughflow: impacts of winds, waves and eddies. *J. Geophys. Res. Oceans*, 127(4). https://doi.org/10.1029/2021JC018133

Prihatiningsih, I., Jaya, I., Atmadipoera, A.S. & Zuraida, R. 2021. Stratification and characteristic of water masses in Selayar Slope-Southern Makassar Strait. *Omni-Akuatika*, 17(1): 27-36. https://doi.org/10.20884/1.oa.2021.17.1.620

Putra, I.W.S.E., Atmadipoera, A.S., Manik, H.M., Harsono, G. & Purwandana, A. 2025. Oceanographic characteristics in the three international Indonesian Archipelago Sea Lanes (IASLs) region: implications for underwater acoustics system. *J. Ilmiah Perik. Kel.*, 17(2): 322-357. https://doi.org/10.20473/jipk.v17i2.56045

Ratnasari, S.L., Harahap, S.A., Sunarto, Purba, N.P. & Pranowo, W.S. 2017. Variabilitas ENSO terhadap arus dan sebaran ikan cakalang (*Katsuwonus pelamis*) di Wilayah Pengelolaan Perikanan 713. *J. Harpodon Borneo*, 10(2): 23-37. https://doi.org/10.35334/harpodon.v10i2.215

Safitri, M., Cahyarini, S.Y. & Putri, M.R. 2012. Variasi arus Arlindo dan parameter oseanografi di Laut Timor sebagai indikasi kejadian ENSO. *J. Ilmu Teknol. Kel. Tropis*, 4(2): 369-377. https://doi.org/10.29244/jitkt.v4i2.7800

Santoso, A., McPhaden, M.J. & Cai, W. 2017. The defining characteristics of ENSO extremes and the strong 2015/2016 El Niño. *Rev. Geophys.*, 55(4): 1079-1129. https://doi.org/10.1002/2017RG000560

Sidabutar, H.C., Rifai, A. & Indriyanti, E. 2014. Kajian lapisan termoklin di lapisan Perairan Utara Jayapura. *J. Oseanog.*, 3(2): 135-141.

Song, T., Xu, G., Yang, K., Li, X. & Peng, S. 2024. Convformer: a model for reconstructing ocean subsurface temperature and salinity fields based on multi-source remote sensing observations. *Rem. Sens.*, 16(13): 2422. https://doi.org/10.3390/rs16132422

Sprintall, J. & Révelard, A. 2014. The Indonesian Throughflow response to Indo-Pacific climate variability. *J. Geophys. Res. Oceans*, 119(2): 1161-1175. https://doi.org/10.1002/2013JC009533

Suhana, M.P. 2018. Karakteristik sebaran menegak dan melintang suhu dan salinitas Perairan Selatan Jawa. *Dinamika Maritim*, 6(2): 9-11.

Suryadarma, M.W., Atmadipoera, A.S., Nugroho, D., Naulita, Y., Zuraida, R. & Apriansyah. 2025. Indonesian Throughflow water and its circulation in the Maluku Sea: an evaluation using the CROCO model. *Reg. Stud. Mar. Sci.*, 82: 104047. https://doi.org/10.1016/j.rsma.2025.104047

Thuillier, O., Le Josse, N., Olteanu, A.-L., Sevaux, M. & Tanguy, H. 2024. Catalogue of coastal-based instances with bathymetric and topographic data. *Earth Syst. Sci. Data*, 16(10): 4529-4556. https://doi.org/10.5194/essd-16-4529-2024

Tian, Z., Wang, C., Yu, Z., Liu, H., Lin, P. & Li, Z. 2024. Tide simulation in a global eddy-resolving ocean model. *Hai Yang Xue Bao*, 43(9): 1-10. https://doi.org/10.1007/s13131-024-2352-5

Toding, J.E., Widagdo, S. & Bintoro, R.S. 2022. Variabilitas temperatur permukaan laut, salinitas, dan curah hujan pada periode El Niño-Southern Oscillation (ENSO) di Perairan Selat Madura. *J. Riset Kel. Tropis*, 4(1): 52-66. https://doi.org/10.30649/jrkt.v4i1.60

Trisnakusumawati, D.D., Sujiono, E.H. & Palloan, P. 2022. Pola sebaran konvektif berdasarkan indeks konvektif dan konvergensi di Sulawesi Selatan. *J. Fisika Unand*, 11(4): 515-522. https://doi.org/10.25077/jfu.11.4.515-522.2022

Triyulianti, I., Radiarta, I.N., Yunanto, A., Pradistya, N.A., Islami, F. & Putri, M.R. 2018. Sistem karbon laut di Perairan Laut Maluku dan Laut Sulawesi. *J. Fisher. Mar. Res.*, 2(3): 192-207. https://doi.org/10.21776/ub.jfmr.2018.002.03.8

Vinayachandran, P.N.M., Masumoto, Y., Roberts, M.J., Huggett, J.A., Halo, I., Chatterjee, A., Amol, P., Gupta, G.V.M., Singh, A., Mukherjee, A., Prakash, S., Beckley, L.E., Raes, E.J. & Hood, R. 2021. Reviews and syntheses: physical and biogeochemical processes associated with upwelling in the Indian Ocean. *Biogeosciences*, 18(22): 5967-6029. https://doi.org/10.5194/bg-18-5967-2021

Wahyuni, D.S., Kisnarti, E.A., Permatasari, I.N. & Adrianto, D. 2024. Vertical characteristic of water mass in the Flores Sea: the effect of the ITF on the transitional season. *IOP Conference Series: Earth and Environmental Science*, 1350(1): 012008. https://doi.org/10.1088/1755-1315/1350/1/012008

Wei, G., Xingyu, S., Xiaowei, C., Yanyu, H., Sudong, Z., Haixia, F., Chenchen, X. & Benjun, M. 2025. Variation of surface chlorophyll-a concentration from 2003-2023 in the tropical western Pacific in response to the ENSO diversity. *J. Mar. Syst.*, 252: 104150. https://doi.org/10.1016/j.jmarsys.2025.104150

Yang, F., Zhang, L. & Long, M. 2022. Intensification of Pacific trade wind and related changes in the relationship between sea surface temperature and sea level pressure. *Geophys. Res. Lett.*, 49(8): p.e2022GL098052.. https://doi.org/10.1029/2022GL0980 52

Yuliardi, A.Y., Prayogo, L.M. & Joesidawati, M.I. 2022. Dinamika distribusi spasial-vertikal massa air di jalur barat dan timur Arlindo pada musim barat. *Jurnal Miyang: Ronggolawe Fisher. Mar. Sci. J.*, 2(2): 38-46. https://doi.org/10.55719/jmiy.v2i2

Zhang, S., Wang, J., Jiang, H., Wang, H. & Yuan, D. 2023. Effects of Indian Ocean Dipole initialization on the forecasting of La Niña 1 year in advance. *Clim. Dyn.*, 61(9-10): 4661-4677. https://doi.org/10.1007/s00382-023-06816-5

Zhu, Q. & Wang, C. 2024. Contributions of Indo-Pacific forcings to interannual variability of the Indonesian Throughflow in the upper and lower layers. *J. Geophys. Res. Oceans*, 129(1): e2023JC020306. https://doi.org/10.1029/2023JC020306